

# Soil thermal properties at Kalpakkam in coastal south India

K ANANDAKUMAR<sup>1</sup>, R VENKATESAN<sup>2</sup>, THARA V. PRABHA<sup>1</sup>

<sup>1</sup>*Crop and Soil Sciences, University of Georgia, 1109 Experiment Street, Griffin, Georgia 30223, USA.*

<sup>2</sup>*Health and Safety Division, SHINE group, IGCAR, Kalpakkam, India.*

Time series of soil surface and subsurface temperatures, soil heat flux, net radiation, air temperature and wind speed were measured at two locations in Kalpakkam, coastal southeast India. The data were analysed to estimate soil thermal diffusivity, thermal conductivity, volumetric heat capacity and soil heat flux. This paper describes the results and discusses their implications.

## 1. Introduction

Soil heat flux is an important component of the surface energy balance of arid, bare or thinly vegetated soil surfaces. Accurate estimates of the soil thermal parameters and soil heat flux are important for numerical modeling studies involving surface energy balance. Such estimates are, however, not easily available. The purpose of this paper is to report a study carried out at Kalpakkam, located on the south east coast of India. Using measured soil temperature and soil heat flux, site specific thermal parameters are estimated. The soil heat flux was estimated using Horton and Wierenga's (1983) procedure and compared with the measurements. The variation of thermal parameters due to wetting of the surface was also studied. Different aspects of diurnal variation of the soil heat flux in relation to the net radiation were also determined.

## 2. Method and measurement

The equation describing the conductive heat transfer in a one-dimensional isotropic medium is

$$\frac{\partial T}{\partial t} = \alpha \frac{\partial^2 T}{\partial z^2}, \quad (1)$$

where  $T$  is the soil temperature,  $\alpha$  is the soil thermal diffusivity,  $t$  the time and  $z$  the depth;  $\alpha$  is

related to thermal conductivity  $\lambda$  and volumetric heat capacity  $C_s$  through the relation

$$\alpha = \lambda/C_s \quad (2)$$

Horton *et al* (1983) evaluated six methods based on the Fourier series representation of  $T$ . We have used all the six methods to estimate  $\alpha$  using the time series measurements made at the experiment site. Thermal conductivity is also estimated.

Traditionally, thermal conductivity is either measured directly using thermal conductivity probes or estimated from the known values of thermal diffusivity and volumetric heat capacity using equation (2). Similarly, volumetric heat capacity is estimated from the knowledge of soil porosity and the soil mineral, organic and water content. However, the measurement probes or detailed soil data are not routinely available and in such situations, indirect estimation methods have to be employed. Massman (1992) developed a method to estimate volumetric heat capacity and thermal conductivity using the analytical expressions derived by van Wijk and De Vries (1963). We have used Massman's method to compute  $C_s$  and  $\lambda$ .

Micrometeorological measurements were carried out at two locations in Kalpakkam (12° N, 82° E), south of Madras, for a period of 10 days (11th February – 20th February, 1998). The first location (L1) was nearly 800 m inland and the second location (L2) was nearly 5 km inland from the coast.

**Keywords.** Soil temperature, thermal conductivity, thermal diffusivity, soil heat flux.

The soil composition at L1 is a mixture of clay, sand and organic materials, where as at L2 the clay content is dominant. Measurements were done at the first location for the first two days and at the second location for the remaining 8 days. The variables measured consisted of net radiation, air temperature, soil surface and subsurface temperatures, soil heat flux and wind speed. Net radiation was measured at a height of 1 m above the surface using a pyrriadiometer (Schenk model -8111, Austria). Soil heat flux was measured at two depths (2 cm and 10 cm) using heat flux plates (HFT-3 Soil heat flux plates, REBS, Campbell Scientific, Inc.). Surface temperature and subsurface temperatures at 7 depths (1, 2, 5, 10, 15, 20 and 50 cm) were measured using Chromel-Alumel thermocouples. All the above data were sampled at 1 s interval and 15 minute average were stored in a datalogger (CR10, Campbell Scientific, Inc.). Temperature sensors and heat flux plates were installed by carefully making holes of the required size parallel to the surface. In the discussion below, only the days with the full 24 h period data are considered for the analysis, thus limiting the data to only one day from site L1 and 5 days from site L2.

### 3. Results and discussion

The diurnal variation of the measured soil temperature profile, one each from the two locations, are presented in figure 1(a) and 1(b). Also shown are measured net radiation, air temperature and wind speed. The peak in surface temperature is attained around 12:00 noon at both the locations and is above  $50^{\circ}\text{C}$ . The maximum surface temperature at L2 is nearly  $5^{\circ}\text{C}$  higher than that at L1. The soil temperature at subsequent depths reaches the peak at different timings, with the time lag increasing with depth. The temperature at 50 cm remained almost constant around  $32^{\circ}\text{C}$  with little diurnal variation. Similar features are noticed on other days at L2, except on 19th February. The area surrounding the soil sensors at L2 were watered on 18th February evening, allowing the water to penetrate to an appreciable depth, down the soil. This experiment was done in order to get an understanding about the soil thermal parameters and the soil heat fluxes of wet surfaces. The diurnal soil temperature variations along with the measured net radiation, air temperature and wind speed for 19th February at L2 are given in figure 2. The figure shows that the maximum daytime surface temperature is reduced by about  $20^{\circ}\text{C}$  than the dry surface value at the same location (figure 1). The temperature gradient between the consecutive levels also has decreased considerably. The observed low temperature during the daytime is due to the fact that

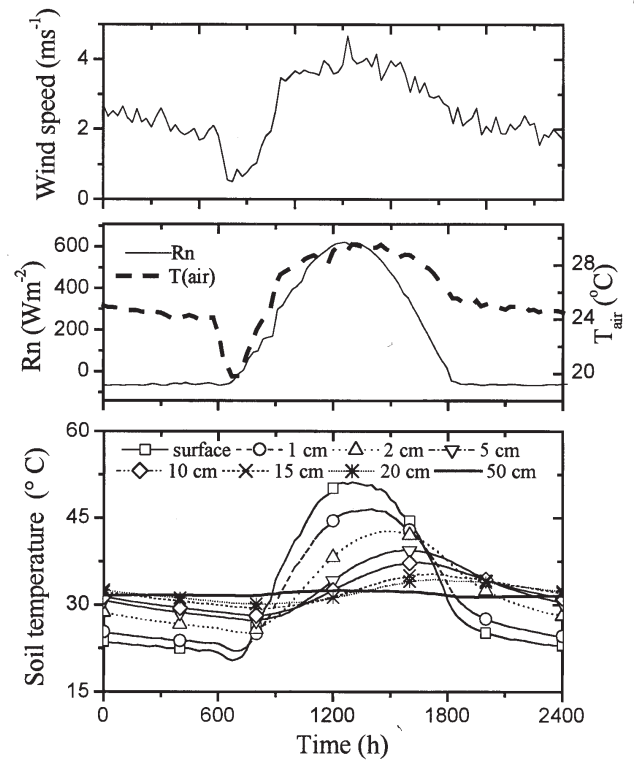


Figure 1(a). Diurnal variation of surface and sub-surface soil temperature profile, net radiation, wind speed and air temperature at location 1 on 12th February.

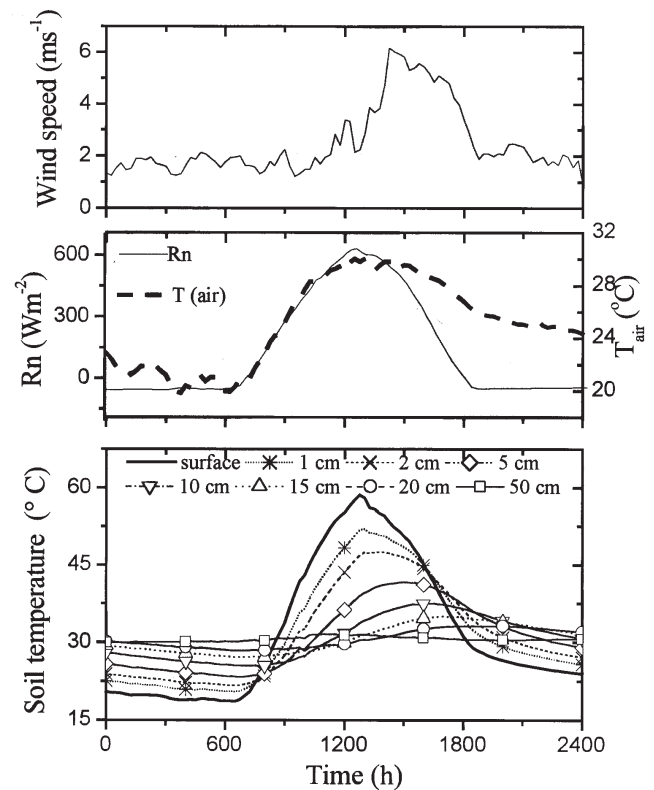


Figure 1(b). Diurnal variation of surface and sub-surface soil temperature profile, net radiation, wind speed and air temperature at location 2 on 14th February.

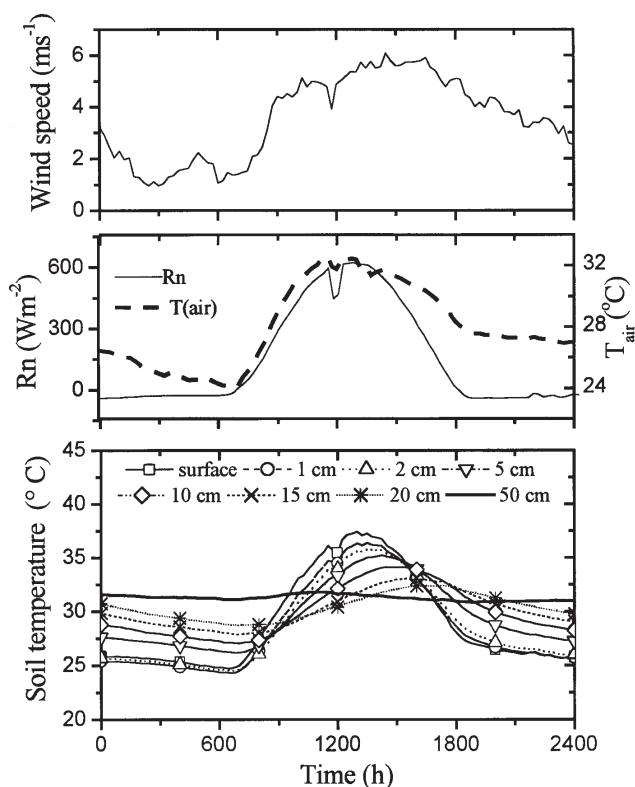


Figure 2. Diurnal variation of surface and sub-surface soil temperature profile, net radiation, wind speed and air temperature at location 2 on 19th February for a wet soil surface.

part of the radiant energy at the surface is utilized for the evaporation of the moisture available at the surface. As a result of this latent heat energy loss, the energy available for heating the soil surface is reduced. The heat capacity and conductivity of the wet soil is higher than the dry soil. This also contributes to the low observed temperature.

Thermal diffusivity ( $\alpha$ ) was calculated for the top 10 cm of the soil using the 6 different methods of Horton *et al* (1983). The results of  $\alpha$  estimations for all the six days studied using all the 6 methods for the top 10 cm soil layer are presented in table 1. It is seen that, in general, there is good agreement between the different methods. The estimations obtained using the first 4 methods show more deviation from that obtained using numeric method and harmonic method. The first four methods use the minimum number of temperature observations for the calculations and that may be the reason for the large deviation. The numerical and harmonic methods show good agreement with each other.

The  $\alpha$  values at L1, corresponding to February 12th, are slightly lower than the values at L2. The soil composition at L1 is a mixture of clay, sand and organic materials, whereas at L2 the clay content is dominant. This could be the reason for the slightly lower values obtained at L1. From February 14th to 17th, at L2,  $\alpha$  values show a decreasing trend. This feature is very clear in almost all the 6 estimations and could be due to the gradual day by day drying up of the soil layer. The value obtained for 19th February, the day corresponding to the wet soil surface, is more than two times larger than other days and is obtained using all methods. This result gives a feeling about the difference in thermal diffusivities of wet and dry soil surfaces.

In the above analysis it is assumed that the soil layer is homogeneous and could be true since the thickness considered is only 10 cm. As we go down to deeper layers, it is possible that the soil thermal properties differ from the top layer due to the difference in composition of the soil and change

Table 1. Estimated values of soil thermal diffusivity using the six methods. For estimation using the amplitude equation, the maximum and minimum temperature measurements at 1 and 10 cm depths were used whereas for the phase equation, the interval between occurrences of maximum temperatures at 1 and 10 cm were employed. Estimates of  $\alpha$  using the arctangent and logarithmic method was achieved using temperature measurement at every 6 h at 1 cm and 10 cm depths. The numerical method estimations were based upon the half hourly temperature measurements during the 24 h period at 4 depth levels: 1, 5, 10 and 15 cm. The measured temperatures at 1, 5 and 15 cm were used to estimate the temperature at 10 cm and was compared with the measured 10 cm temperature to obtain the correct choice of  $\alpha$ . In the harmonic analysis, the 1 cm hourly temperature observations are employed to obtain the amplitude and phase of the first two harmonics.

Date	Amplitude equation $\times 10^{-7} \text{ m}^2 \text{ s}^{-1}$	Phase equation $\times 10^{-7} \text{ m}^2 \text{ s}^{-1}$	Arctangent equation $\times 10^{-7} \text{ m}^2 \text{ s}^{-1}$	Logarithmic equation $\times 10^{-7} \text{ m}^2 \text{ s}^{-1}$	Numerical method $\times 10^{-7} \text{ m}^2 \text{ s}^{-1}$	Harmonic equation $\times 10^{-7} \text{ m}^2 \text{ s}^{-1}$
February 12	2.50	3.51	2.77	2.22	4.20	3.46
February 14	3.28	4.07	5.32	3.34	5.80	5.50
February 15	2.90	6.88	4.15	2.87	5.10	4.68
February 16	3.04	4.77	3.68	2.86	5.00	4.60
February 17	3.00	5.68	3.60	2.98	5.10	4.52
February 19 (wet surface)	10.6	19.1	10.4	10.2	12.5	13.7

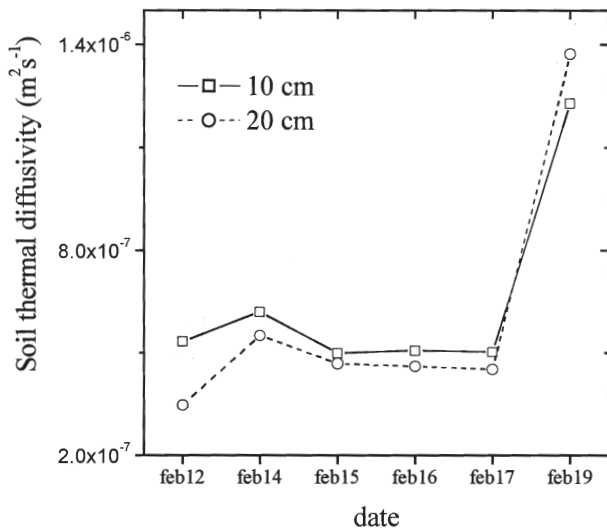


Figure 3. Estimated thermal diffusivity for 10 cm and 20 cm soil depth levels.

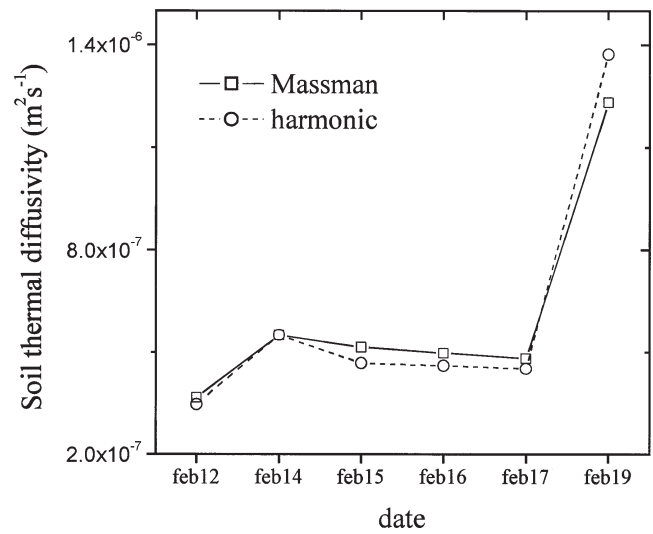


Figure 4. Comparison of thermal diffusivity estimated using harmonic and Massman's method.

Table 2. Estimated values of soil thermal conductivity and heat capacity.

Date	Thermal conductivity $Wm^{-1}K^{-1}$	Volumetric heat capacity $\times 10^6 Jm^{-3}K^{-1}$
February 12	0.518	1.413
February 14	0.675	1.228
February 15	0.625	1.213
February 16	0.605	1.215
February 17	0.592	1.232
February 19 (wet surface)	2.148	1.745

in water content. To get an understanding about the variation of  $\alpha$  with depth,  $\alpha$  was estimated using the harmonic method and the 20 cm temperature measurements. The values obtained for all the six days are plotted in figure 3 along with the values obtained using 10 cm temperature measurements, for comparison. It can be seen that for all the first 5 days, the  $\alpha$  estimations using 20 cm temperature are higher than the 10 cm counterpart whereas for the wet soil (February 19th) it is slightly smaller. The reason for the higher values obtained for the first five days is due to the presence of more moisture content at deeper levels, and  $\alpha$  increases with moisture content. The presence of more moisture content at deeper levels was noticed while digging for installing the sensors. In the case of the wet soil, it was artificially watered and it is possible that the water content at the top levels are more than at deeper levels and could be the reason for the slightly smaller value.

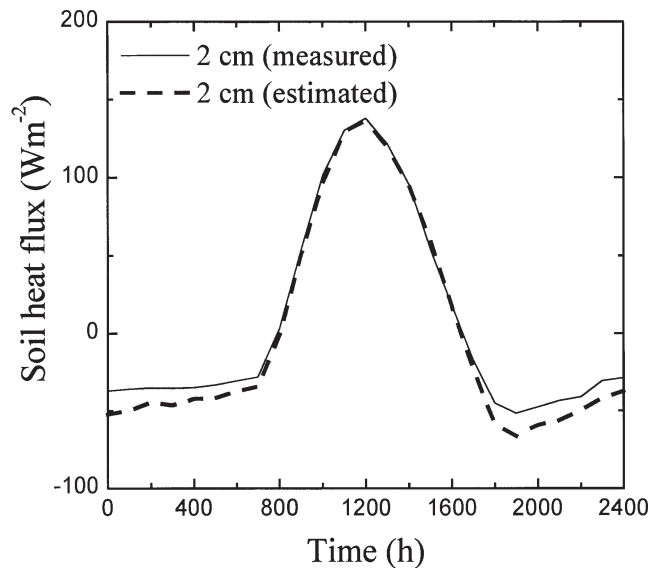


Figure 5. Diurnal variation of measured and estimated soil heat flux at 2 cm for 15th February.

$C_s$  and  $\lambda$  were estimated following Massman's method. The values are given in table 2. The  $\lambda$  value at L1 (February 12th) is slightly smaller than the first four day values at L2. This could be due to the different soil composition at L1. The  $\lambda$  values at L2 show variations similar to that of  $\alpha$  and again could be due to the drying up of soil. Here also, the wet soil thermal conductivity is nearly 3 times higher than the dry cases. The  $C_s$  values exhibit slightly complex behaviour. The value at L1 is higher than the first four-day values at L2. At L2, there is no clear trend on first 4 days, and for the wet surface, it is higher than the dry days at L2 and L1.

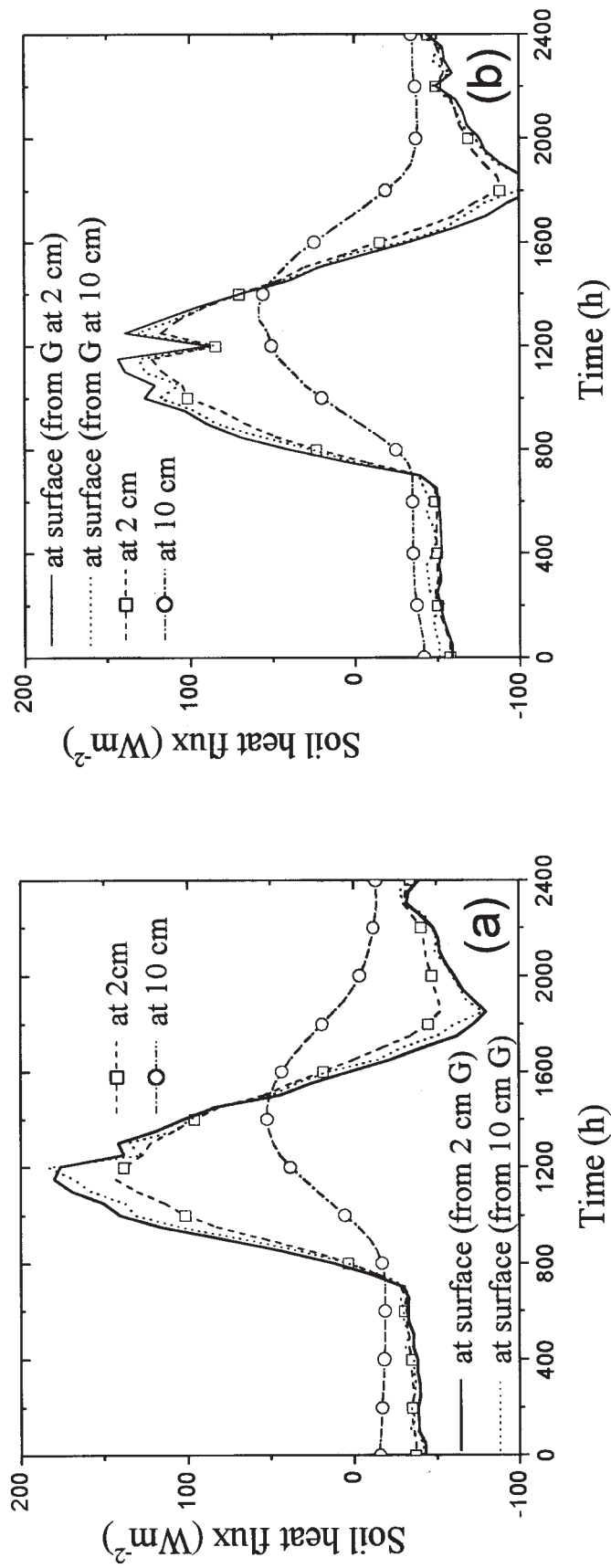


Figure 6. Diurnal variation of soil heat flux at the surface estimated from the 2 cm and 10 cm measurements and the measured fluxes at 2 cm and 10 cm: (a) on 15th February and (b) on 19th February (wet surface).

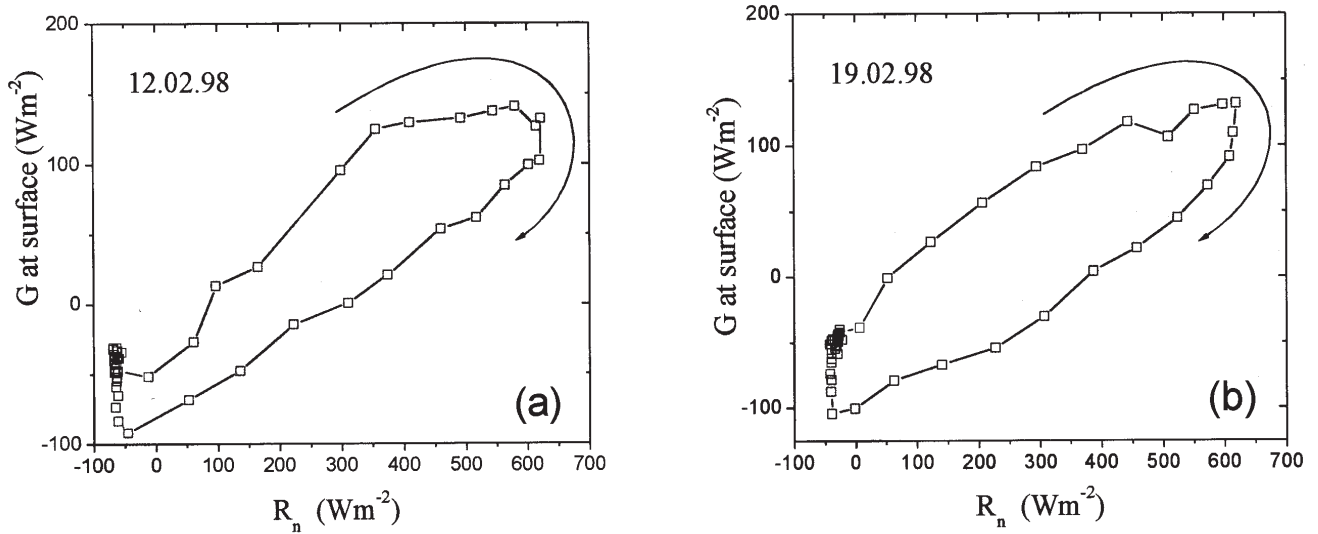


Figure 7. Variation of soil heat flux at the surface with net radiation: (a) on 12th February and (b) on 19th February.

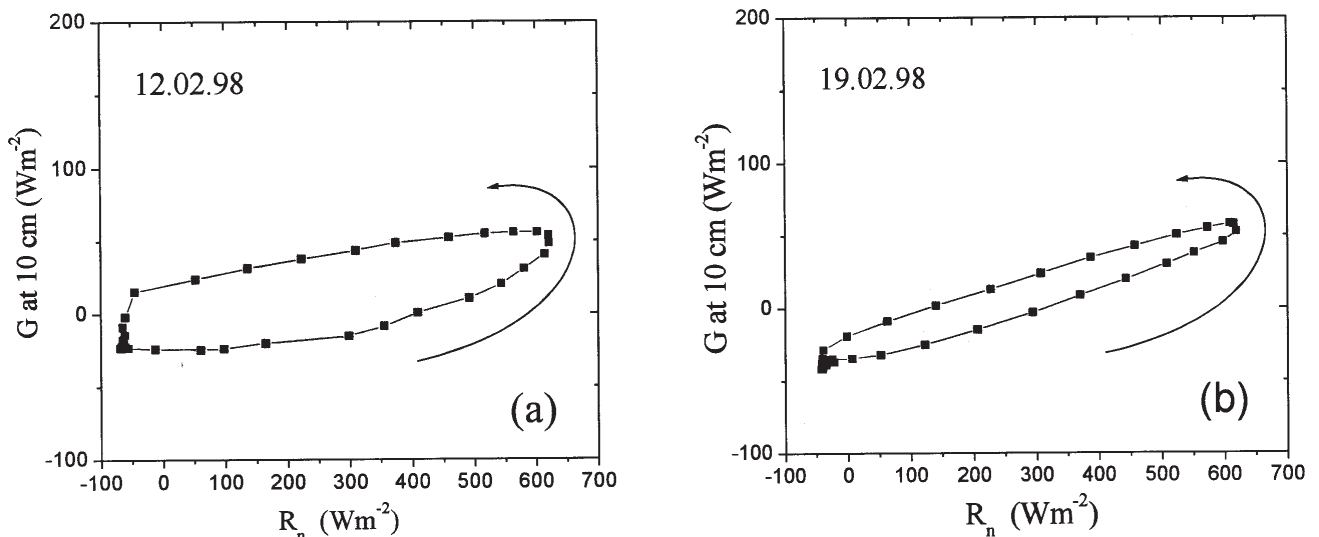


Figure 8. Variation of soil heat flux at 10 cm with net radiation: (a) on 12th February and (b) on 19th February.

$\alpha$  was also determined indirectly from the estimated values of  $\lambda$  and  $C_s$  using equation (2). These agreed closely with those obtained using the harmonic method (figure 4), which indicates the reliability of the latter.

The soil heat flux at 2 cm was estimated based on the harmonic method of Horton and Wierenga (1983) using the temperature observations at 2 cm and the estimated values of  $\alpha$  and  $C_s$ . The amplitude and phase of 10 harmonics estimated from the hourly 2 cm temperature observations were used to estimate the heat flux. The  $C_s$  values (table 2) determined using Massman's method and the  $\alpha$  values estimated using harmonic method were employed for the estimations. Figure 5 shows the diurnal variations of measured and estimated

soil heat flux at 2 cm depth for 15th February. It can be seen that there is very good agreement between the measured and estimated fluxes.

The soil heat flux at the surface can be computed from the measurements at 2 cm and 10 cm using the equation given by Braud *et al* (1993)

$$G = G_z + C_s \Delta_z \frac{\left( T_s^{t_1} - T_s^{t_0} + \frac{(\Delta T_s^{t_0} - \Delta T_s^{t_1})}{2} \right)}{\Delta t} \quad (3)$$

where  $C_s$  is the volumetric heat capacity,  $\Delta t$  (= 30 minutes) is the time interval,  $G_z$  is the observed heat flux at depth  $z$ ,  $t_0$  and  $t_1$  are two consecutive time steps,  $\Delta T_s$  is the temperature difference between the surface and depth  $z$ .

The heat flux obtained at the surface both from 2 cm and 10 cm measurements are shown in figure 6 for 2 days (15th and 19th February) along with the measured fluxes at 2 and 10 cm. It is clear from the figure that both the estimated values are in close agreement to each other for all the days studied. This result also illustrates the homogeneity of the top 10 cm of the soil layer as the same  $C_s$  value is used for both the estimations. It can also be noticed from the figure that there exists a phase lag between the flux peaks at different depths and is attributed to the time required for the heat to penetrate down the soil. A similar pattern is noticed in temperature profile also (figure 1). The mean of the soil heat flux estimated from both the depths were used for further analysis.

The variation of soil surface heat flux ( $G$ ) with net radiation ( $R_n$ ) is given in figure 7 for 2 days. It can be seen that, instead of a straight line relationship, a clockwise loop behaviour is observed indicating that the soil heat flux, for the same amount of net radiation is higher during the warming phase (morning hours) than the cooling phase (afternoon hours). Again, on 12th February (L1, dry surface), the maximum in  $G$  is reached before  $R_n$  attained the peak. This is because as the soil surface is heated up, the temperature difference between the surface and air increases and an appreciable amount of heat is transferred to the overlying atmosphere in the form of sensible and latent heat flux. Because of this, during cooling phase, the amount of radiant energy available to be transformed into  $G$  is less compared to the warming phase. In the case of wet surface (February 19th, figure 7b), similar clockwise behaviour is obtained, but the peak in  $G$  is attained at the same time corresponding to the peak in  $R_n$  and the magnitude of the peak is smaller than the dry cases. Two factors lead to this difference: i) appreciable amount of energy is lost to the atmosphere in the form of latent heat and ii) the conductivity and heat capacity of the soil is enhanced due to the presence of moisture content.

In contrast to the above,  $G$  vs.  $R_n$  for the measured  $G$  at 10 cm shows anti-clockwise loop behaviour (figure 8). Also, for dry soil cases, the peak in  $G$  is attained after  $R_n$  reached the maximum. The said features are due to the fact that during the warming phase, it takes some time for the heat to

penetrate deep into the soil. During the cooling phase, the changes taking place at the surface are not immediately reflected few centimeters below the surface and reduction  $G$  is slow. In the case of wet surface, however, the peak in  $G$  and  $R_n$  are reached almost at the same time and the anti-clockwise loop is more steep and its width is less. This is mainly due to the enhanced thermal conductivity of the soil which supports the heat flow down the soil relatively fast.

### Acknowledgments

The authors gratefully acknowledge the contributions for the field experiment from Prof. Erich Mursch-Radlgruber and Rengarajan, Institute for Meteorology and Physics, Agricultural University of Vienna, Austria. The first author (AK) would like to acknowledge the Indira Gandhi Centre for Atomic Research for providing the opportunity to participate in the experiment. The authors acknowledge the keen interest and incessant support from A R Sundararajan, Head, Health and Safety Division, AERB and Dr. A Natarajan, Head, Health and Safety Division, IGCAR. The authors are indebted to the reviewers for many useful comments.

### References

- Braud I, Noilhan J, Bessemoulin P and Mascart P 1993 Bare ground surface heat and water exchanges under dry conditions: observations and parameterization; *Boundary-Layer Meteorol.* **66** 173–200
- Horton R and Wierenga P J 1983 Estimating the soil heat flux from observations of soil temperature near the surface; *Soil Sci. Soc. Am. J.* **47** 14–20.
- Horton R, Wierenga P J and Nielsen D R 1983 Evaluation of methods for determining the apparent thermal diffusivity of soil near the surface; *Soil Sci. Soc. Am. J.* **47** 25–32
- Massman W J 1992 Correcting errors associated with soil heat flux measurements and estimating soil thermal properties from soil temperature and heat flux plate data; *Agric. For. Meteorol.* **59** 249–266
- Van Wijk W R and de Vries D A 1963 Periodic temperature variations in a homogeneous soil. In: W R van Wijk (ed), *Physics of plant environment*, (Amsterdam: North-Holland) 382 pp.